

Is signal efficiency affected by interference between muons in the tracker, possibly in a way that is not well-modeled by Monte Carlo?

Jim Pivarski

February 27, 2011

1 Dominant efficiency systematic

The dominant efficiency systematic for nearby muons (inverse boost $1/\gamma \lesssim 0.3$) is from confusion of segments from different muons in the muon system. The uncertainty in this inefficiency is quantified in Fig. 5 of AN-2010/462: there is a 2% difference between crossing and non-crossing muons for leading $p_T > 15$ GeV/ c , averaged uniformly in η , and 6% at the $|\eta| = 2.4$ extreme. (Definitions and supporting information are in Appendix A.) The cause of the inefficiency is due to incorrectly assigned segments: every muon track in the analysis is required to match at least two *unique* segments, and if muon A takes muon B 's segments while muon B does not match to muon A 's, then muon B would fail to be identified. Distances between extrapolated tracks and muon segments are typically 1–10 cm due to multiple scattering between the tracker and the muon system, so segments may even be confused for opening angles as large as 0.3 rad. The effect is larger in the endcap because large entrance angles in the magnetic field bending plane help to distinguish muons in the barrel.

Track-finding efficiencies are much higher than muon-identification efficiencies: $\sim 99.8\%$ for $p_T > 5$ GeV/ c , $|\eta| < 2.4$ tracks compared with $\sim 97\%$ for muons with the same kinematics. Since there are no road-broadening effects in the tracker that are comparable to the multiple scattering in the CMS magnet return yoke, tracks must be much closer together to suffer inefficiencies in the tracker alone. In this document, I will explicitly quantify this effect with Monte Carlo and information from

- *Commissioning and Performance of the CMS Pixel Tracker with Cosmic Ray Muons*, <http://arxiv.org/abs/0911.5434>;
- *Commissioning and Performance of the CMS Silicon Strip Tracker with Cosmic Ray Muons*, <http://arxiv.org/abs/0911.4996>;
- *CMS Tracking Performance Results from early LHC Operation*, <http://arxiv.org/abs/1007.1988>.

I will also compare data and Monte Carlo distributions of the $\phi(1020)$ resonance, which allows us to test the simulation with $0.05 < \Delta R < 0.15$ opening angles.

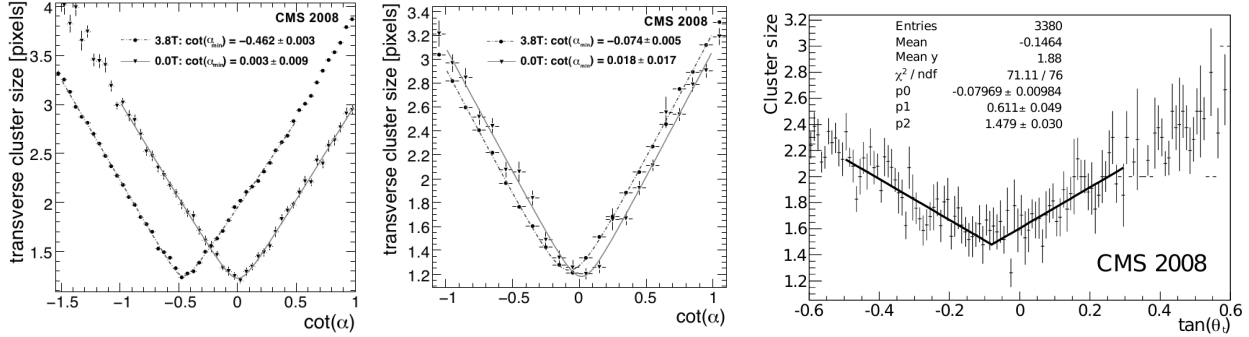


Figure 1: Cluster size versus entrance angle in the pixel barrel (left), pixel endcap (middle), with and without magnetic field, and TOB layer 4 (right). High- p_T tracks have minimal entrance angle.

2 CMS track reconstruction procedure

The CMS track reconstruction proceeds in five iterations, though the last three are designed for $p_T < 0.9$ GeV/ c and displaced tracks (low pixel efficiency). The first two iterations search for continuations of pairs and triplets of pixel clusters, and only if clusters can be unambiguously associated with a track (“highPurity”) are they removed from the list of clusters available in subsequent iterations. Tracks found in the same iteration can share up to 50% of their clusters. Clusters may be interpreted differently as hits on different tracks, due to track-dependent corrections, but inclusion of a cluster on one track does not automatically disqualify it from another.

3 Criteria for 50% overlap

To produce tracks that overlap through $\sim 50\%$ of the tracker, two oppositely signed muons would need to have very high momentum. To estimate this momentum, we use the following facts:

- pixel channels are 100–150 μm wide (assume 100),
- TOB strips are about three times as wide (assume 300),
- clusters are 1.5–2 channels wide for high- p_T tracks.

The first two facts come from a conversation with Kevin Burkett, the last comes from Fig. 8 and 11 of the pixel and strip CRAFT papers, reproduced in Fig. 1. Cluster size depends primarily on path length through the silicon, with a near-minimum for high- p_T tracks (near-minimal because of the magnetic field).

Figures 2 and 3 quantify the degree of separation at two distances from the beamline: 5 cm (first pixel layer) and 60 cm (first TOB layer, about 50% through the tracker). Two trajectories were propagated from the origin to 5 and 60 cm cylinders using the appropriate CMSSW propagator for a variety of $\Delta\phi$ opening angles at the origin and initial p_T of both

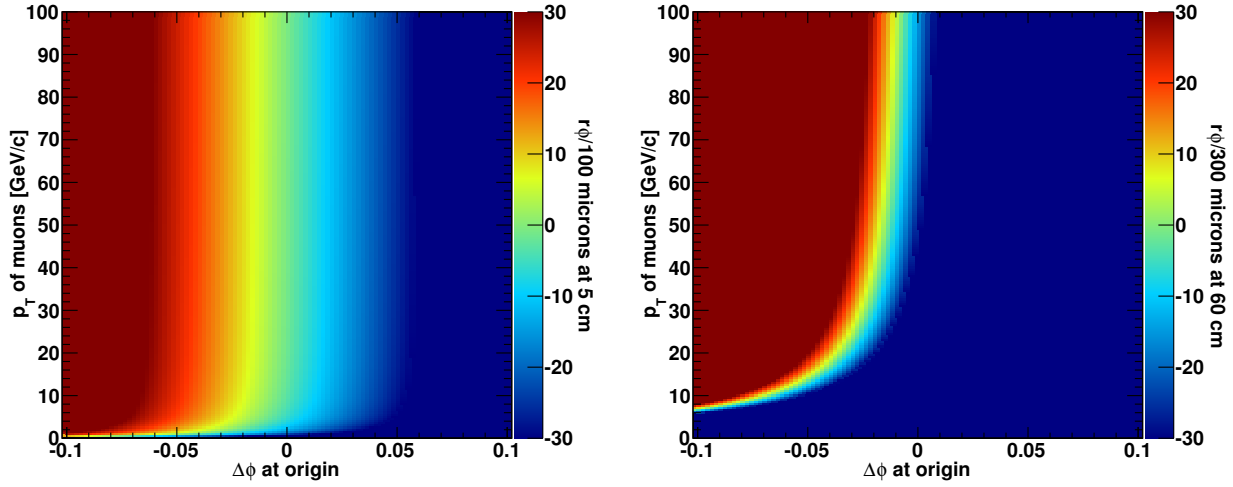


Figure 2: Separation of two muon trajectories at the first pixel layer, 5 cm from the beamline (left), and the first TOB layer, 60 cm from the beamline (right). The color scale is the $r\phi$ distance between the muon trajectories on a cylinder of the given radius, measured in units of channel widths, taking $100\text{ }\mu\text{m}$ for the pixel and $300\text{ }\mu\text{m}$ for the TOB. Green is zero separation; red and blue are 30 channels apart. The $r\phi$ separation asymptotically approaches a constant multiple of $\Delta\phi$ at the origin for high- p_T muons (both muons have the same p_T in this simulation).

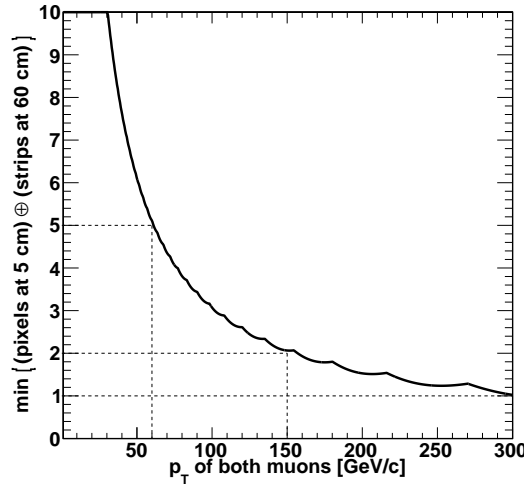


Figure 3: Minimum separation in *both* the pixel detector at a radius of 5 cm *and* the TOB at a radius of 60 cm. The vertical axis is the minimum $r\phi$ separation in pixel channel widths, added in quadrature with the minimum $r\phi$ separation in TOB channel widths, minimized over possible values of $\Delta\phi$ at the origin. For two muons to be separated by ~ 1 channel width in the pixel *and* TOB, both muons would need about $p_T \approx 300\text{ GeV}/c$.

trajectories (both momenta were equal, with $\eta = 0$). For a ~ 5 channel width separation at both radii, both muons would need $p_T > 60$ GeV/ c , for ~ 2 channel widths, both muons would need $p_T > 150$ GeV/ c , and for ~ 1 channel width, both muons would need $p_T > 300$ GeV/ c .

4 Observing track interference in pair-gun MC

To search for the onset of an inefficiency due to nearby tracks in the tracker, I plotted efficiency versus ΔR using our pair-gun MC. The pair-gun MC is a full CMSSW simulation of two opposite-sign muons with uniformly random pair momentum ($0 < p_T^{\mu\mu} < 100$ GeV/ c), mass ($2m_\mu < m < 6$ GeV/ c^2), pseudorapidity ($-2.5 < \eta^{\mu\mu} < 2.5$), and azimuthal angle ($-\pi < \phi^{\mu\mu} < \pi$). Each pair of muons is reconstructed three times: once with the μ^+ as the only particle in the event, once with the μ^- as the only particle in the event, and once with both μ^+ and μ^- in the same event. This allows us to study efficiency losses due to interference separately from single-particle efficiency.

With these tools, we can define “interference efficiency” in the following way:

$$P(\mu^+\mu^-|\mu^+ \text{ and } \mu^-) = \frac{\text{both muons reconstructed in the same event and separately}}{\text{both muons reconstructed separately}} \quad (1)$$

with additional generator-level requirements of $p_T > 5$ GeV/ c and $|\eta| < 2.4$ for both numerator and denominator. “Reconstructed” means that the reconstructed track exists with ≥ 8 hits and $\chi^2/N_{\text{dof}} < 4$, though these quality cuts have negligible impact on the final result. The probability of reconstructing both muons separately, given kinematical acceptance, is 99.6%.

Figure 4 presents this interference efficiency as a function of ΔR , where an 8% dip is visible for $\Delta R < 0.01$. This dip is correlated with high momentum (same figure), suggesting that it is related to track overlap. For context, we show the mass distribution of muon pairs with $\Delta R < 0.01$ in this sample in Fig. 5. The 100 GeV/ c upper limit in momentum implies only mass < 0.5 GeV/ c^2 pairs have such a small opening angle. For a 1 GeV/ c^2 boson, the onset of the effect would be at higher momenta.

The same study can be performed for the full muon cuts, that is, adding the requirement that the track is reconstructed as a TrackerMuon with ≥ 2 arbitrated muon segments. This is presented in Fig. 6. The interference efficiency for the full muon cuts has the same shape as a function of ΔR , though a lower plateau for $\Delta R \gg 0.01$. This is the effect of the muons crossing the muon system (discussed in the analysis note), which is not a strict function of ΔR at the origin.

5 Data/MC comparisons for tracking

The *CMS Tracking Performance Results from early LHC Operation* paper (<http://arxiv.org/abs/1007.1988>) presents a detailed overview of the status of the tracking simulation with early collisions. The simulation is shown to reproduce the shapes of signal responses (see Fig. 7, copied from the paper) and many high-level tracking quantities. Figure 8 shows the number of hits and χ^2/N_{dof} distributions from this paper, which are relevant to our

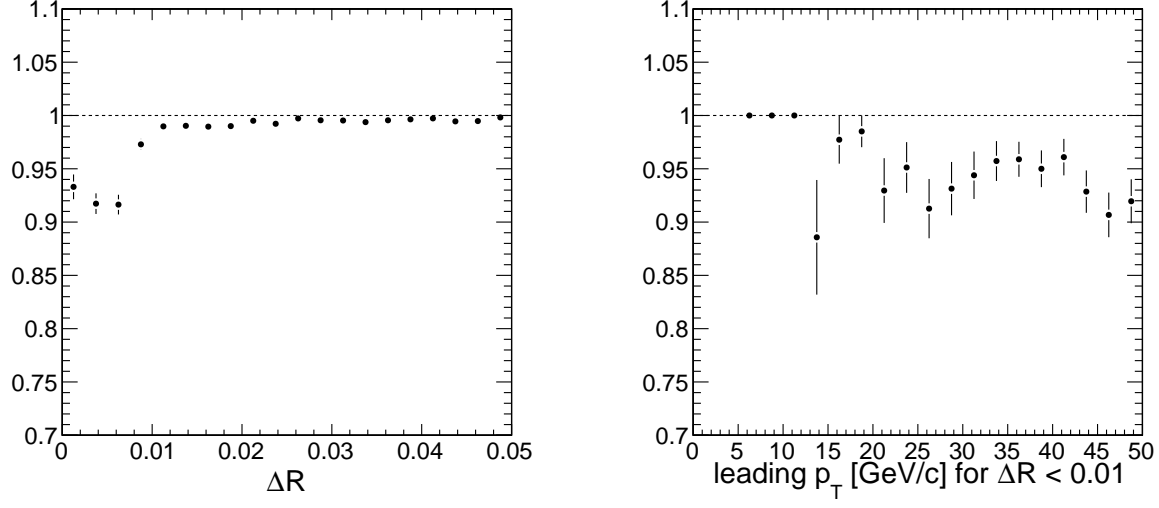


Figure 4: Left: $P(\mu^+\mu^-|\mu^+ \text{ and } \mu^-)$ for track cuts (see text) versus ΔR . Right: the same quantity versus leading muon p_T for $\Delta R < 0.01$, showing that the effect prefers high momenta.

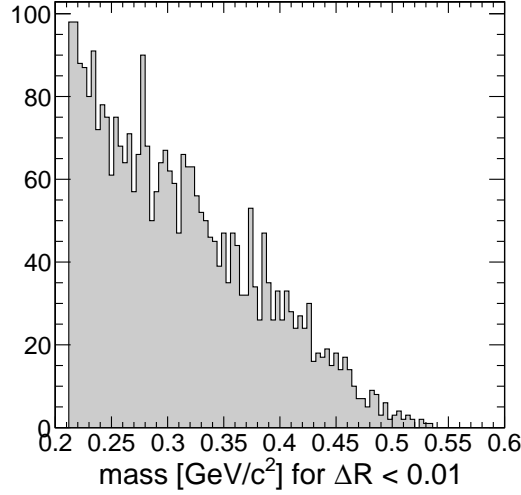


Figure 5: Values of muon pair mass consistent with $\Delta R < 0.01$ in this simulation, for context.

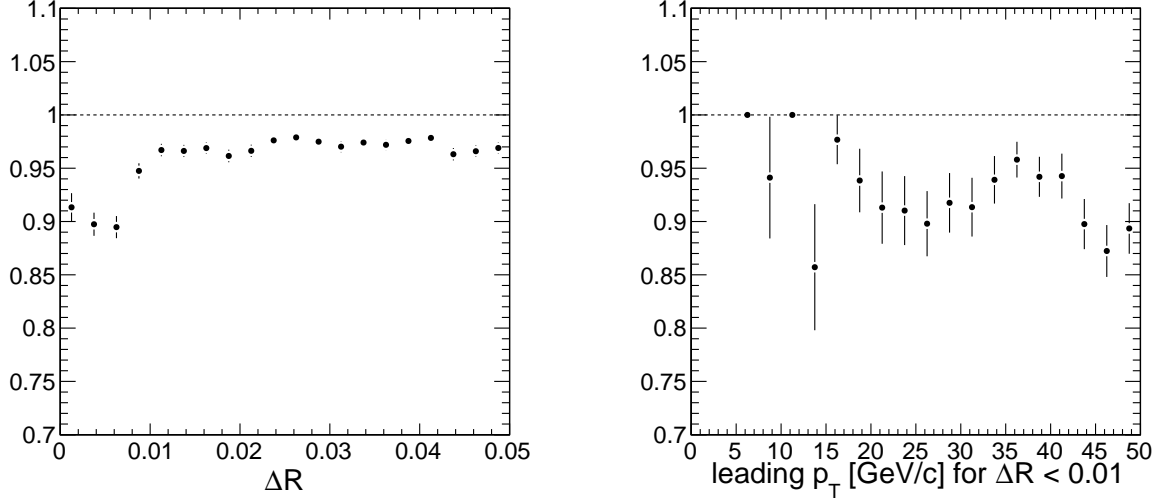


Figure 6: Left: $P(\mu^+\mu^-|\mu^+ \text{ and } \mu^-)$ for muon cuts versus ΔR . Right: the same quantity versus leading muon p_T for $\Delta R < 0.01$, showing that the effect prefers high momenta.

analysis as track quality cuts. The distributions in the early LHC paper represent low- p_T hadrons, rather than $p_T > 5$ GeV/ c muons, though.

One may argue that the tracking simulation may be trusted if it reproduces all low-level signals and has a realistic alignment, since our analysis signal only differs in geometry, and all geometry and algorithms are the same for data and Monte Carlo. This can be partially tested with studies of the $\phi(1020)$ resonance.

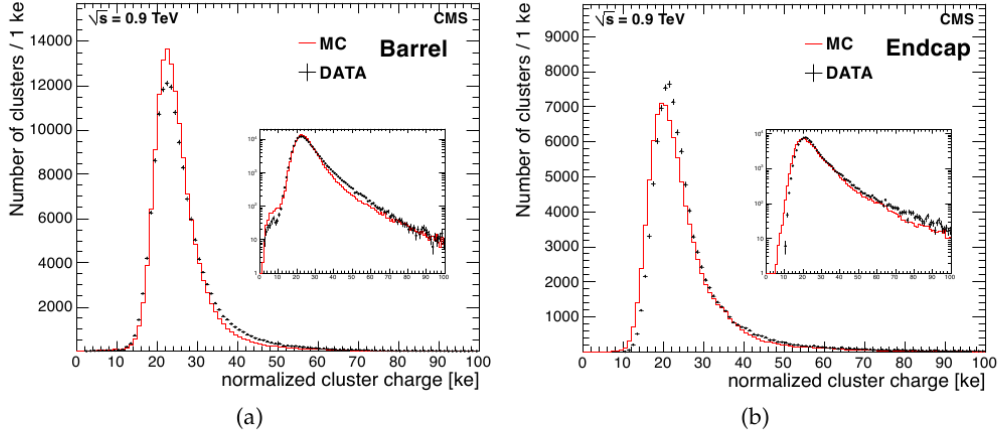
6 Study of the $\phi(1020)$ resonance

The $\phi(1020)$ resonance provides a standard candle of low-mass, moderately high-momentum dimuons with which to test the level of data/MC agreement. It corresponds to a moderately low range of opening angles $0.05 < \Delta R < 0.15$, though not low enough to sample the $\Delta R < 0.01$ tracker inefficiency. It is the lowest-mass Standard Model narrow resonance found in both data and Monte Carlo ($\omega(782) \rightarrow \mu\mu$ is missing from the Pythia 6 decay tables), and it is in the middle of the target mass range of our analysis, though lower than our target momentum range.

Figure 9 presents the invariant mass distribution near the $\phi(1020)$ peak, indicating the signal region ($|m - m_\phi| < 0.025$ GeV/ c^2), the sidebands ($0.050 < |m - m_\phi| < 0.075$ GeV/ c^2), and a pure $\phi(1020)$ Monte Carlo simulation. The $\phi(1020)$ simulation is a subset of InclusiveMu5-Pt30 (muons from Pythia 6 QCD): dimuons selected at generator level to have $\phi(1020)$ as their parent.

The $\phi(1020)$ events in Monte Carlo are all prompt and in jets, while the data has a displaced component and an isolated component. For a more appropriate comparison, I applied the following cuts:

- distance between the dimuon vertex and the closest primary vertex in z must be less than 1 mm ($L_{xy} < 1$ mm);



~~Figure 4:~~ The normalized cluster charge measured in the (a) barrel and (b) endcap pixel detectors for the sample of 0.9 TeV minimum bias events. The insets show the same distributions on semi-log scales.

Figure 7: Figure reproduced from the early LHC tracking paper.

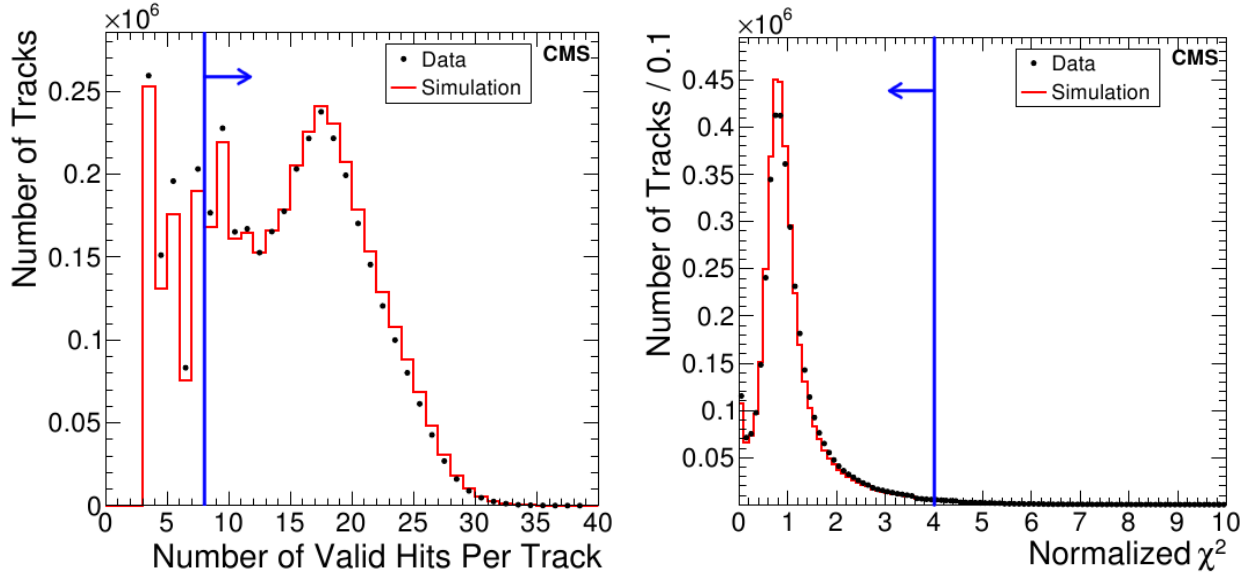


Figure 8: Two figures from the early LHC tracking paper relevant to our analysis: blue lines indicate our cuts. These distributions have different shapes for our $p_T > 5$ GeV/ c tracks.

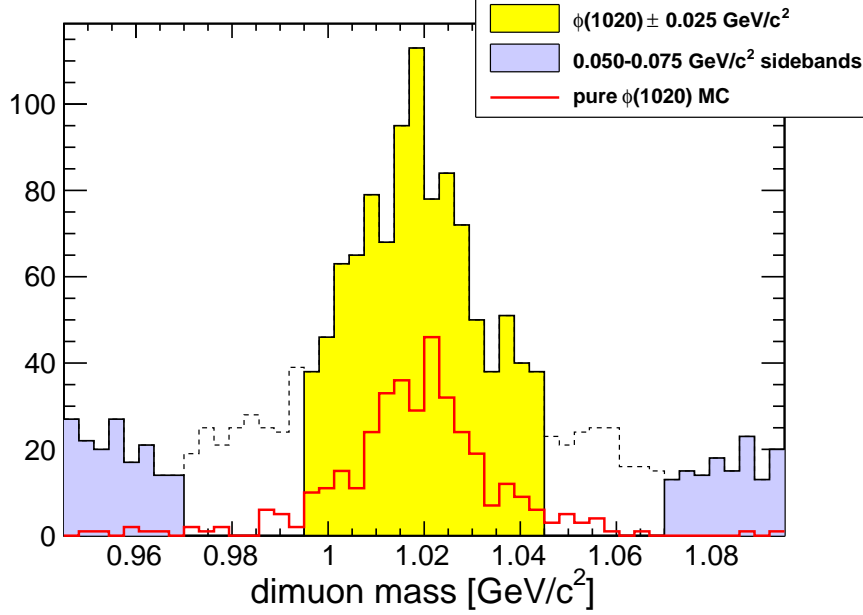


Figure 9: Basic distribution of the $\phi(1020)$ study: dimuon invariant mass distribution of data (dashed line, colored in sections) with the signal region indicated by yellow, the sidebands indicated by blue, overlaid with a pure $\phi(1020)$ MC simulation (unscaled).

- the sum of track p_T for $p_T > 1.5$ GeV/ c in a $\Delta R < 0.4$ cone around the dimuon axis must be greater than 3 GeV/ c ($I_{so} > 3$ GeV/ c);
- exactly two reconstructed muons per event;
- apply $|m - m_\phi| < 0.025$ GeV/ c^2 to Monte Carlo as well as the signal;
- at least one muon must have $p_T > 10$ GeV/ c .

The data were collected using any single or double-muon trigger that was available. Prescales changed during the run, but HLT_Mu9 and HLT_Mu11 were prescaled late in the year—the requirement of $p_T > 10$ GeV/ c is a compromise between strict correctness (our analysis uses only $p_T > 15$ GeV/ c) and the need to maximize the size of the dataset for statistically meaningful comparisons. Figure 10 shows sideband-subtracted $\phi(1020)$ data overlaid by normalized Monte Carlo of the highest and lowest- p_T muon in each event. The data and Monte Carlo p_T spectra are consistent: there is no evidence of trigger prescale thresholds in the spectrum. Figure 11 presents the ΔR , η , I_{so} , and L_{xy} distributions (with all cuts applied).

Figure 12 shows the same sideband-subtracted data overlaid by normalized Monte Carlo for the distributions used to define muon quality cuts: number of tracker hits, tracker χ^2/N_{dof} , and number of arbitrated muon segments. All cuts are far from the distributions except the number of segments. The number of segments matched to a TrackerMuon track depends on the level of agreement between tracks propagated from the tracker and muon segment positions and entrance angles, which are shown in Fig. 13.

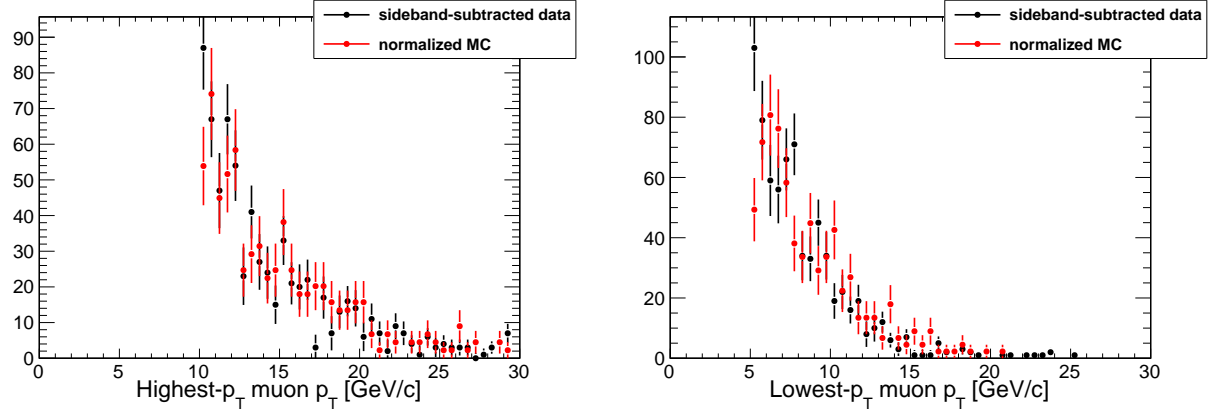


Figure 10: Sideband-subtracted muon momentum distributions overlaid by Monte Carlo (normalized to equal number of events).

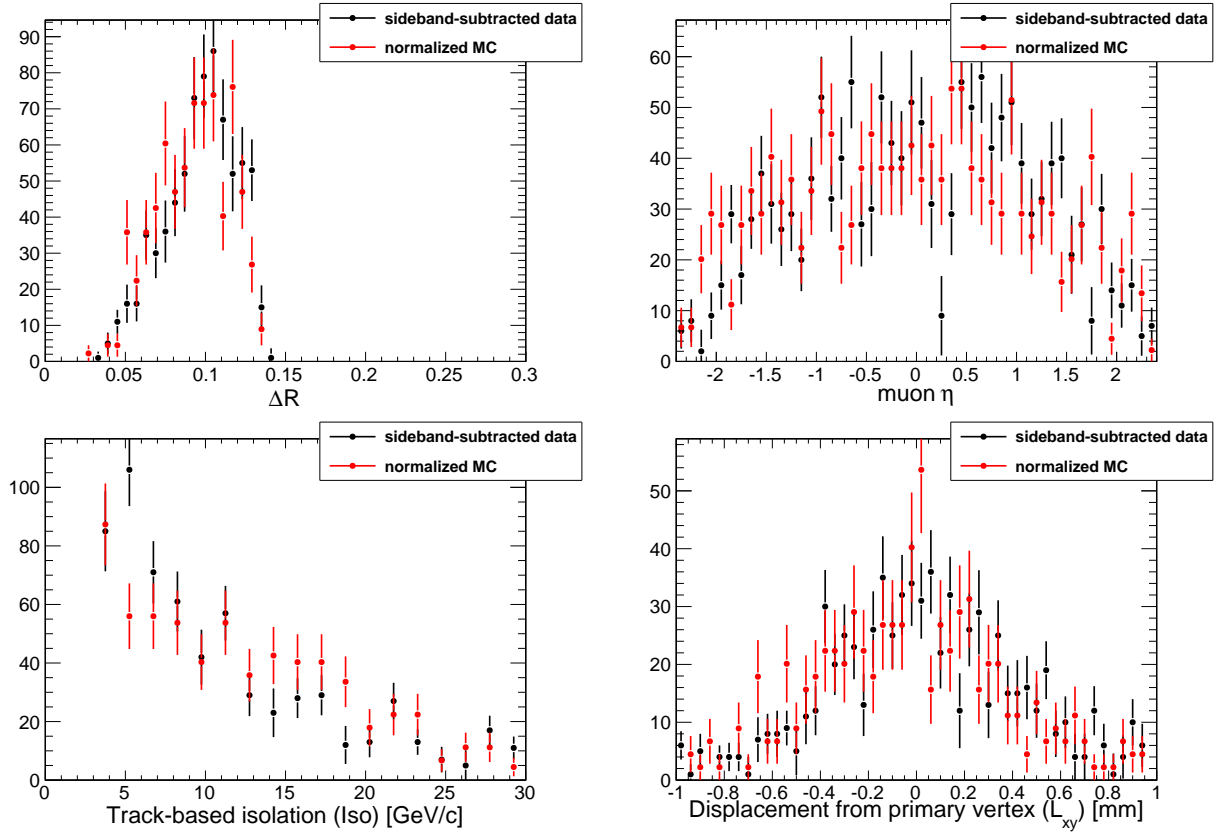


Figure 11: Other distributions relevant for or used to define the $\phi(1020)$ sample.

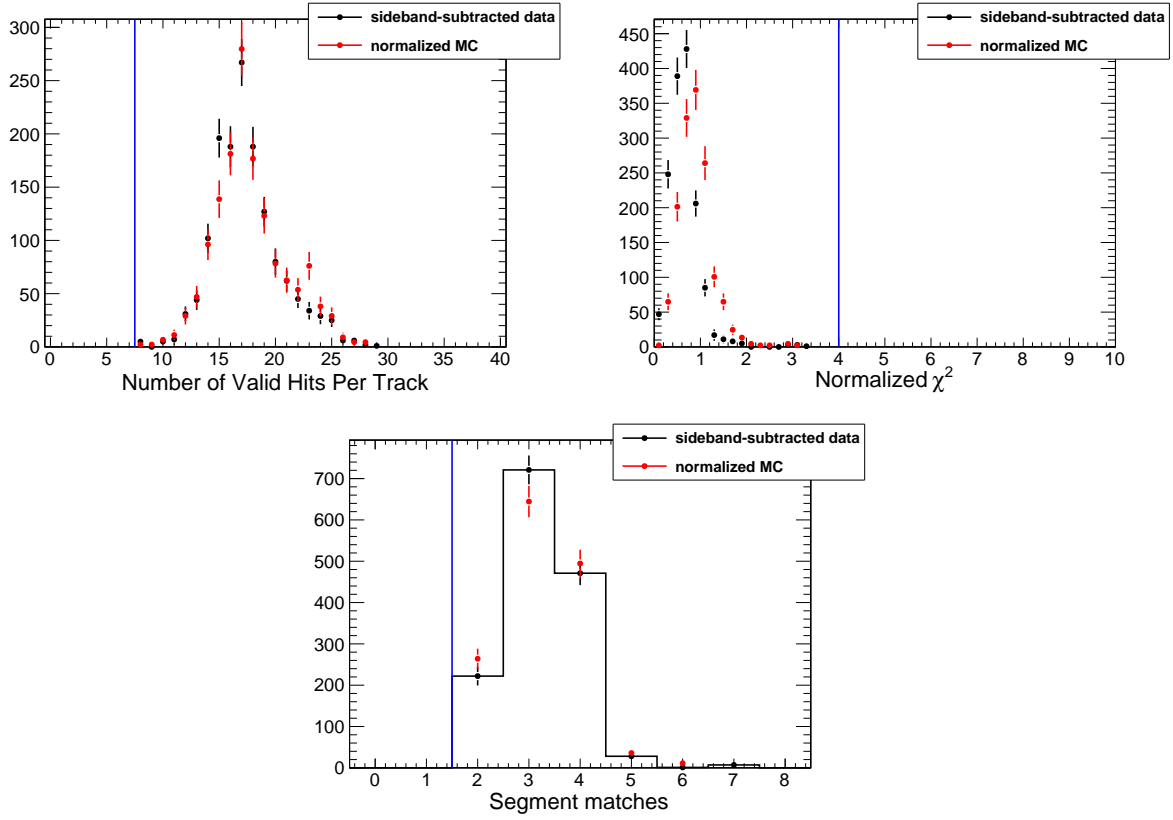


Figure 12: Distributions of track quality cuts (top row) and muon quality cuts (bottom) with cut thresholds indicated in blue. All cuts have been applied in all distributions.

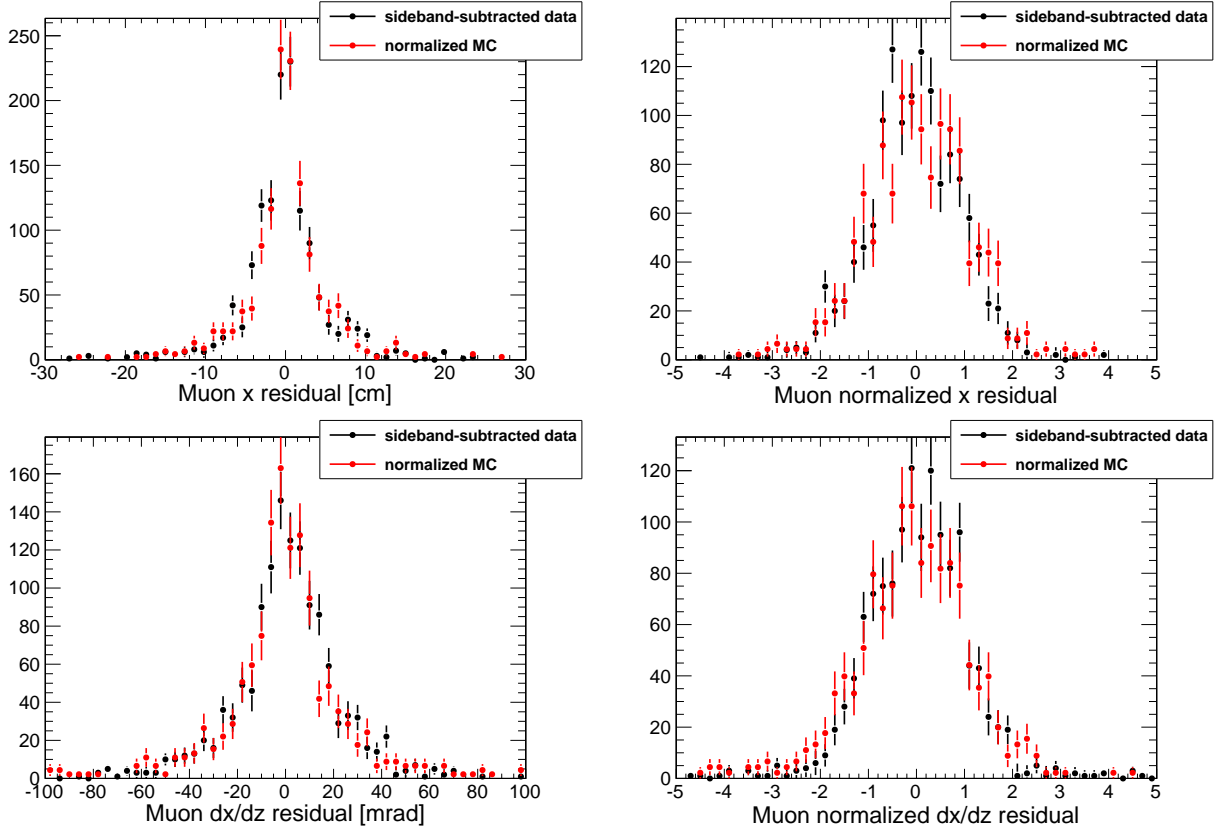


Figure 13: Distance between propagated track and muon segment in the magnetic field bending plane (x , top-left), the same normalized by uncertainty (top-right), the difference in entrance angle (dx/dz , bottom-left), and the same normalized by uncertainty (bottom-right). These are relevant for determining the number of muon segments matched to a TrackerMuon.

The Monte Carlo sample used in this study and all signal samples used in the main analysis were produced using ideal alignment and calibration conditions. The data in this $\phi(1020)$ study is a combination of Sep17ReReco (2010A) and PromptReco (2010B), unlike the main analysis, which uses Dec22ReReco. The only observed discrepancy between data and Monte Carlo is in the χ^2/N_{dof} distribution (Fig. 12 top-right), in which the Monte Carlo peaks at one but the data peaks lower than one. This *could* be because the tracker alignment uses artificially inflated Alignment Position Errors (APEs) in PromptReco for safety (this was the case in early LHC running... not sure if it's still true... **FIXME**). The muon residuals distributions (Fig. 13) are completely insensitive to muon alignment conditions for ~ 20 GeV/ c muon momenta because of the dominance of multiple scattering in the propagation.

7 Conclusions

Muon segment assignment for muons whose trajectories cross in the muon system is the dominant efficiency systematic for a wide range of opening angles. However, efficiency losses in the tracker could play a significant role for 150–300 GeV/ c muons. An 8% loss in efficiency is observed in pair-gun MC for $\Delta R < 0.01$ muon pairs, though such a high boost is a special case in our analysis. The simulation was tested for moderately low opening angles ($0.05 < \Delta R < 0.15$) using the $\phi(1020)$ resonance, though the region where the tracker begins to be inefficient for nearby muons is orthogonal to this or any test using Standard Model resonances.